

\mathcal{T}, \mathcal{P} -odd effects in the LuOH⁺ cation.

Daniel E. Maison,^{1,*} Leonid V. Skripnikov,^{1,2,†} Gleb Penyazkov,^{1,2,‡} Matt Grau,^{3,§} and Alexander N. Petrov^{1,2,¶}

¹*Petersburg Nuclear Physics Institute named by B.P. Konstantinov of National Research Center “Kurchatov Institute” (NRC “Kurchatov Institute” - PNPI),*

¹*Orlova roscha mcr., Gatchina, 188300 Leningrad region, Russia***

²*Saint Petersburg State University, 7/9 Universitetskaya nab., St. Petersburg, 199034 Russia*

³*Department of Physics, Old Dominion University, Norfolk, VA 23529*

The LuOH⁺ cation is a promising system to search for manifestations of time reversal and spatial parity violation effects. Such effects in LuOH⁺ induced by the electron electric dipole moment e EDM and the scalar-pseudoscalar interaction of the nucleus with electrons, characterized by k_s constant, in LuOH⁺ are studied. The enhancement factors, polarization in the external electric field, hyperfine interaction, rovibrational structure are calculated. The study is required for the experiment preparation and extraction of the e EDM and k_s values from experimental data.

INTRODUCTION

For a long time, it was supposed, that the laws of physics should satisfy the conditions of the invariance with respect to charge conjugation (\mathcal{C}), spatial parity (\mathcal{P}) and time reversion (\mathcal{T}) symmetries. However, in the second half of XXth century it was experimentally confirmed, that both \mathcal{P} - and combined \mathcal{CP} -symmetries are violated in weak interactions. According to the \mathcal{CPT} theorem, violation of \mathcal{CP} is equivalent to violation of \mathcal{T} symmetry. The search for the new manifestations of violation of these symmetries is one of the topical sections of modern theoretical and experimental physics [1]. For example, \mathcal{CP} -violation is of great interest for cosmology and astrophysics, since it is one of three necessary conditions of baryogenesis [2].

One of the approaches to search for simultaneous violation of \mathcal{T} and \mathcal{P} symmetries (\mathcal{T}, \mathcal{P} -violation) is the determination of elementary particles electric dipole moments (EDMs) [3]. For example, the recent refinement of the neutron EDM upper constraint [4] led to the updated constraint of the quantum chromodynamics (QCD) parameter $\bar{\theta}$ [5]. In addition, the electron electric dipole moment (e EDM) can be also used as indicator of \mathcal{T}, \mathcal{P} -violation in the standard model (SM) and the physics beyond it. The latest result of the ACME collaboration in 2018 allowed one to obtain the strongest constraint on e EDM $|d_e| \lesssim 1.1 \cdot 10^{-29} e \cdot \text{cm}$ [6]. It overcame the previous constraints [7, 8] by almost an order of magnitude, and led to strong restrictions for various SM extensions. According to estimates within the SM, e EDM value is ten orders of magnitude lower [9, 10], so there is still room for more precise experiments to search for new physics before encountering the SM background.

Recently it was suggested to perform e EDM search experiments using linear triatomic molecules [11, 12]. In Ref. [11], it was noted, that, due to the l -doubling effect in the first excited bending mode $\nu_2 = 1$, the linear triatomic molecules, such as YbOH, can be completely polarized by relatively weak electric field, $\sim 100\text{V/cm}$

¹. More importantly, these molecules can be successfully cooled [14]. These facts allow one to increase experimental sensitivity to e EDM and other \mathcal{T}, \mathcal{P} -odd effects.

As it was demonstrated in Ref. [8], molecular cations can also be used for the e EDM determination. While experiments with ions suffer from reduced count rates, they are advantaged by long interrogation times afforded by the ion trap. The constraint $|d_e| \lesssim 1.3 \cdot 10^{-28} e \cdot \text{cm}$ obtained in this experiment is only an order of magnitude weaker, than the current one. This fact demonstrates, that the updated e EDM restrictions can possibly be obtained in ion trap experiments.

Combining these two ideas, it was suggested to consider the LuOH⁺ molecular ion for \mathcal{T}, \mathcal{P} -odd effects search [15], as it can be formed from Lu atomic ions (which can be laser-cooled [16]), and once formed it can be sympathetically during an experiment cooled by co-trapped atomic ions. It has an electronic structure similar to YbOH. However, as it has been shown [15], the LuOH⁺ molecular cation can be even more sensitive to the nuclear \mathcal{CP} -violation effects, than YbOH, owing to the large electric quadrupole moment of ¹⁷⁶Lu.

In a polar molecule with an atom of a heavy element, the \mathcal{T}, \mathcal{P} -violating energy shift associated with e EDM and the scalar-pseudoscalar nucleus-electron interaction characterized by the dimensionless coupling constant k_s reads

$$\Delta E_{\mathcal{P}, \mathcal{T}} = P (E_{\text{eff}} d_e + E_s k_s). \quad (1)$$

The \mathcal{T}, \mathcal{P} -violating energy shift induced by e EDM in a molecule is determined by the following Hamiltonian [17, 18]:

$$H_d^{\text{eff}} = d_e \sum_a 2ic\gamma_a^0 \gamma_a^5 \mathbf{p}_a^2, \quad (2)$$

¹ However, later it was pointed out, that for some states the maximal polarization is only 50% and no one state get 100% polarization [13].

index a runs over electrons (as in all equations below), \mathbf{p} is the momentum operator for an electron and γ^0 and $\gamma^5 = -i\gamma_0\gamma_1\gamma_2\gamma_3$ are the Dirac matrices, defined according to Ref. [19]². For a linear molecule this interaction can be characterized by the molecular constant W_d :

$$W_d = \frac{1}{\Omega} \langle \Psi | \frac{H_d}{d_e} | \Psi \rangle. \quad (3)$$

In these designations effective electric field introduced in Eq. (1) acting on the electron electric dipole moment is $E_{\text{eff}} = W_d|\Omega|$. Another considered source of \mathcal{T}, \mathcal{P} -violation is the scalar-pseudoscalar nucleus-electron interaction given by the following Hamiltonian (see [20], Eq. (130), and also [21]):

$$H_s = i \frac{G_F}{\sqrt{2}} Z k_s \sum_a \gamma_a^0 \gamma_a^5 \rho_N(\mathbf{r}_a), \quad (4)$$

where G_F is the Fermi-coupling constant, Z is the heavy nucleus charge, $\rho_N(\mathbf{r})$ is the nuclear density normalized to unity and \mathbf{r} is the electron radius-vector with respect to the heavy atom nucleus under consideration. This interaction is characterized by the molecular parameter $W_{T,P}$:

$$W_{T,P} = \frac{1}{\Omega} \langle \Psi | \frac{H_s}{k_s} | \Psi \rangle, \quad (5)$$

or $E_s = W_{T,P}|\Omega|$.

It is well known that for diatomics (like ThO, HfF⁺) the polarization P in Eq. (1)³ smoothly approaches unity for small laboratory electric fields due to the existence of Ω -doublet structure [22]. In Ref. [13] we showed, however, that l -doubling structure is in general different from Ω -doubling, and that polarization tends to approach $|P| = 0.5$ value for molecules (like YbOH, LuOH⁺, RaOH, etc.) with Hund's case b coupling scheme. The final value depends on the value of the l -doubling, spin-rotation constant and hyperfine interaction.

Knowing the enhancement coefficients E_{eff} , E_s and P one may extract the value of the constants d_e and k_s from the measured energy shift.

To populate the required $\nu_2 = 1$ level in experiments one needs to know the bending vibrational energy levels structure. Therefore, these calculations are also performed in the present paper. Up to now there is no corresponding experimental information.

ELECTRONIC STRUCTURE CALCULATION DETAILS

The electronic structure calculations were performed within the relativistic coupled cluster approach. It is based on the exponential ansatz of wave function

$$\Psi = \exp(\hat{T}) \Phi, \quad (6)$$

where Φ is the electronic wave function in the Dirac-Hartree-Fock approximation, Ψ is the wave function with electronic correlation taken into account, and \hat{T} is the excitation cluster operator. It can be written as the following series:

$$\hat{T} = \hat{T}_1 + \hat{T}_2 + \hat{T}_3 + \dots, \quad (7)$$

with operators \hat{T}_k defined as:

$$\hat{T}_k = \frac{1}{k!} \sum_{\substack{i_1 < i_2 < \dots < i_k \in \text{occ} \\ b_1 < b_2 < \dots < b_k \in \text{virt}}} t_{i_1 i_2 \dots i_k}^{b_1 b_2 \dots b_k} \hat{a}_{b_1}^\dagger \hat{a}_{b_2}^\dagger \dots \hat{a}_{b_k}^\dagger \hat{a}_{i_1} \hat{a}_{i_2} \dots \hat{a}_{i_k}. \quad (8)$$

Indexes i_{\dots} and b_{\dots} label occupied and virtual electronic states, respectively. Coefficients $t_{\dots}^{b\dots}$ are scalar variables to be defined, also called cluster amplitudes. In the present study, we exploit the relativistic coupled cluster approach with single and double cluster amplitudes (CCSD) and coupled cluster approach with single, double and perturbative triplet amplitudes (CCSD(T)) [23, 24]. The former one exploits the approximation

$$\hat{T} \approx \hat{T}_1 + \hat{T}_2,$$

and the latter one includes also calculation of the energy correction due to \hat{T}_3 [25].

For calculation of the potential energy surface we have used the AE3Z(Lu) \oplus aug-cc-PVTZ-DK(O,H) basis sets [26–28]. At the coupled cluster stage we have excluded 1s..3d electrons of Lu from the correlation treatment and set virtual orbitals energy cutoff equal to 70 Hartree. The calculations of magnetic dipole hyperfine structure constants on hydrogen nucleus (see below), ion-frame electric dipole moment with respect to mass center and spin-rotational constant have been performed within the same procedure, with replacement the basis set aug-cc-PVTZ-DK on hydrogen by the AAE4Z basis set [29]. Calculations of parameters of \mathcal{T}, \mathcal{P} -violation effects in Eq. (1) and electric quadrupole hyperfine constant induced by Lu nucleus have been performed at the CCSD(T) level of theory and using the AE3Z(Lu) \oplus aug-cc-PVTZ-DK(O,H) basis as in Ref. [15]. In these calculations all electrons were included in correlation calculation and virtual energy cutoff was set to 11000 Hartree. The contribution of high-energy orbitals in correlation calculation has been extensively analyzed in Refs. [30, 31]. Calculations of properties have been performed for the equilibrium geometry parameters determined in the present paper.

² Note that in the literature, there are two common definitions of γ_5 which differ by the sign.

³ P in Eq. (1), in general, is not equal to the mean value of the projection of unit vector \hat{z} along molecular axis on direction of the external electric field.

Molecular relativistic CCSD(T) calculations were carried out using the DIRAC [32, 33] program package. Calculation of the property integrals were performed within the code developed in Refs. [34, 35].

ROVIBRATIONAL LEVELS CALCULATION DETAILS

Following Ref. [13] we present our Hamiltonian in molecular reference frame as

$$\hat{\mathbf{H}} = \hat{\mathbf{H}}_{\text{mol}} + \hat{\mathbf{H}}_{\text{hfs}} + \hat{\mathbf{H}}_{\text{ext}}, \quad (9)$$

where

$$\hat{\mathbf{H}}_{\text{mol}} = \frac{(\hat{\mathbf{J}} - \hat{\mathbf{J}}^{e-v})^2}{2\mu R^2} + \frac{(\hat{\mathbf{J}}^v)^2}{2\mu_{OH} r^2} + V(\theta) \quad (10)$$

is the molecular Hamiltonian as it is described in Ref. [13], μ is the reduced mass of the Lu-OH system, μ_{OH} is the reduced mass of the OH, $\hat{\mathbf{J}}$ is the total electronic, vibrational, and rotational angular momentum, $\hat{\mathbf{J}}^{e-v} = \hat{\mathbf{J}}^e + \hat{\mathbf{J}}^v$ is the electronic-vibrational momentum, $\hat{\mathbf{J}}^e$ is the electronic momentum, $\hat{\mathbf{J}}^v$ is the vibrational momentum, R is the distance between Lu and the center mass of OH, r is OH bond length and θ is the angle between OH and the axis (z axis of the molecular frame) directed from Lu to the OH center of mass. The condition $\theta = 0$ corresponds to the linear configuration where the O atom is between Lu and H ones. R , r and θ are the so called Jacobi coordinates, see Fig. (1).

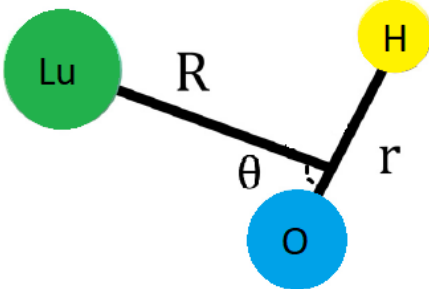


FIG. 1. Jacobi coordinates for LuOH^+ molecule.

In the current work, we have fixed R and r , to their equilibrium values obtained in the electronic structure calculations. In this approximation we neglect the influence of the stretching ν_1 (associated with R) and OH ligand ν_3 (associated with r) modes but nevertheless take into account the bending ones (associated with θ) with fixed R, r . $V(\theta)$ is the potential energy curve obtained in the electronic structure calculations.

$$\begin{aligned} \hat{\mathbf{H}}_{\text{hfs}} = & -g_H I^H \cdot \sum_a \left(\frac{\boldsymbol{\alpha}_{2a} \times \mathbf{r}_{2a}}{r_{2a}^3} \right) + \\ & -g_{\text{Lu}} \mu_N I^{\text{Lu}} \cdot \sum_a \left(\frac{\boldsymbol{\alpha}_a \times \mathbf{r}_{1a}}{r_{1a}^3} \right) \\ & -e^2 \sum_q (-1)^q \hat{Q}_q^2(I^{\text{Lu}}) \sum_a \sqrt{\frac{2\pi}{5}} \frac{Y_{2q}(\theta_{1a}, \phi_{1a})}{r_{1a}^3} \end{aligned} \quad (11)$$

is the hyperfine interaction of electrons with Lu and H nuclei, g_{Lu} and g_H are the g-factors of the lutetium and hydrogen nuclei, $\boldsymbol{\alpha}_a$ are the Dirac matrices for the a -th electron, \mathbf{r}_{1a} and \mathbf{r}_{2a} are their radius-vectors in the coordinate system centered on the Lu and H nuclei, $\hat{Q}_q^2(I^{\text{Lu}})$ is the quadrupole moment operator for ^{175}Lu nucleus, $I^{\text{Lu}} = 7/2$, $I^H = 1/2$ are nuclear spins for ^{175}Lu and H.

The Stark Hamiltonian

$$\hat{\mathbf{H}}_{\text{ext}} = -\mathbf{D} \cdot \mathbf{E} \quad (12)$$

describes the interaction of the molecule with the external electric field, and \mathbf{D} is the dipole moment operator.

Wavefunctions, rovibrational energies and hyperfine structure were obtained by numerical diagonalization of the Hamiltonian (9) over the basis set of the electronic-rotational-vibrational-nuclear spins wavefunctions

$$\Psi_{\Omega m \omega} P_{lm}(\theta) \Theta_{M_J, \omega}^J(\alpha, \beta) U_{M_I^H}^H U_{M_I^{\text{Lu}}}^{\text{Lu}}. \quad (13)$$

Here $\Theta_{M_J, \omega}^J(\alpha, \beta) = \sqrt{(2J+1)/4\pi} D_{M_J, \omega}^J(\alpha, \beta, \gamma = 0)$ is the rotational wavefunction, α, β correspond to azimuthal and polar angles of the z axis, $U_{M_I^H}^H$ and $U_{M_I^{\text{Lu}}}^{\text{Lu}}$ are the hydrogen and lutetium nuclear spin wavefunctions, M_J is the projection of the molecular (electronic-rotational-vibrational) angular momentum $\hat{\mathbf{J}}$ on the lab axis, ω is the projection of the same momentum on z axis of the molecular frame, M_I^H and M_I^{Lu} are the projections of the nuclear angular momenta of hydrogen and lutetium on the lab axis, $P_{lm}(\theta)$ is the associated Legendre polynomial, l is the vibration angular momentum and m is its projection on the molecular axis, $\Psi_{\Omega m \omega}$ is the electronic wavefunction (see Ref. [13] for details).

In this calculation functions with $\omega - m = \Omega = \pm 1/2$, $l = 0 - 30$ and $m = 0, \pm 1, \pm 2$, $J = 1/2, 3/2, 5/2$ were included to the basis set (13). The ground vibrational state $\nu_2 = 0$ corresponds to $m = 0$, the first excited bending mode $\nu_2 = 1$ to $m = \pm 1$, the second excited bending mode has states with $m = 0, \pm 2$ etc. A common designation ν_2^m for vibrational levels will be used below.

Provided that the *electronic-vibrational* matrix elements are known, the matrix elements of $\hat{\mathbf{H}}$ between states in the basis set (13) can be calculated with help of the angular momentum algebra [13, 36] mostly in the same way as for the diatomic molecules [37].

The required matrix elements associated with ^{175}Lu nucleus magnetic hyperfine interaction

$$\begin{aligned} A_{\parallel} &= -\frac{g_{\text{Lu}}}{\Omega} \times \\ &\langle \Psi_{\Omega m \omega} P_{lm} | \sum_a \left(\frac{\boldsymbol{\alpha}_{1a} \times \mathbf{r}_{1a}}{r_{1a}^3} \right)_z | \Psi_{\Omega m \omega} P_{l'm} \rangle \\ &= 8142 \delta_{ll'} \text{ MHz}, \quad (14) \end{aligned}$$

$$\begin{aligned} A_{\perp} &= -g_{\text{Lu}} \times \\ &\langle \Psi_{\Omega=1/2m\omega} P_{lm} | \sum_a \left(\frac{\boldsymbol{\alpha}_a \times \mathbf{r}_{1a}}{r_{1a}^3} \right)_+ | \Psi_{\Omega=-1/2m\omega-1} P_{l'm} \rangle \\ &= 7864 \delta_{ll'} \text{ MHz}, \quad (15) \end{aligned}$$

were taken from Ref. [15].

Matrix elements associated with the hyperfine interaction induced by the H nucleus magnetic

$$\begin{aligned} A_{\parallel} &= -\frac{g_{\text{H}}}{\Omega} \times \\ &\langle \Psi_{\Omega m \omega} P_{lm} | \sum_a \left(\frac{\boldsymbol{\alpha}_a \times \mathbf{r}_a}{r_a^3} \right)_z | \Psi_{\Omega m \omega} P_{l'm} \rangle \\ &= 2.4 \delta_{ll'} \text{ MHz}, \quad (16) \end{aligned}$$

$$\begin{aligned} A_{\perp} &= -g_{\text{H}} \times \\ &\langle \Psi_{\Omega=1/2m\omega} P_{lm} | \sum_i \left(\frac{\boldsymbol{\alpha}_i \times \mathbf{r}_i}{r_i^3} \right)_+ | \Psi_{\Omega=-1/2m\omega-1} P_{l'm} \rangle \\ &= -0.9 \delta_{ll'} \text{ MHz}, \quad (17) \end{aligned}$$

dipole moment operator

$$\langle \Psi_{\Omega m \omega} P_{lm} | D_z | \Psi_{\Omega m \omega} P_{l'm} \rangle = -0.55 \delta_{ll'} \text{ a.u.} \quad (18)$$

determining interaction with the external electric field and $J_+^e = J_x^e + iJ_y^e$

$$\begin{aligned} J_+^e &= \langle \Psi_{\Omega=1/2m\omega} P_{lm} | J_+^e | \Psi_{\Omega=-1/2m\omega-1} P_{l'm} \rangle \\ &= 0.992 \delta_{ll'} \quad (19) \end{aligned}$$

and

$$\begin{aligned} e^2 Q q_0 &= \langle \Psi_{\Omega m \omega} P_{lm} | \\ &e^2 \sum_q (-1)^q \hat{Q}_q^2 (\mathbf{I}^{\text{Lu}}) \sum_a \sqrt{\frac{2\pi}{5}} \frac{Y_{2q}(\theta_{1a}, \phi_{1a})}{r_{1a}^3} \\ &| \Psi_{\Omega m \omega} P_{l'm} \rangle = -5012 \delta_{ll'} \text{ MHz}, \quad (20) \end{aligned}$$

where $Q = 3.49$ barn is the quadrupole moment for the ^{175}Lu nucleus [38, 39], were calculated in the present work. To calculate the \mathcal{T}, \mathcal{P} -odd shifts the average value of corresponding Hamiltonians (2,4) were evaluated.

RESULTS

Electronic structure calculation confirmed the linear equilibrium geometry for LuOH^+ with $R = 1.930 \text{ \AA}$, $r = 0.954 \text{ \AA}$, $\theta = 0$ equilibrium values ⁴. The calculated values of the \mathcal{T}, \mathcal{P} -violation parameters are $E_{\text{eff}} = -29.1 \text{ GV/cm}$, $E_s = -25.7 \text{ kHz}$. In both cases contribution of triple cluster amplitudes is 2.7%. This is slightly larger than this contribution to the W_M parameter calculated for LuOH^+ in Ref. [15].

In Fig. 2 and Table I the calculated potential energy curve and corresponding spectroscopic properties are given. One can see that results for the CCSD and CCSD(T) models are very close to each other. Excitation energy of ν_2 quanta is about 100 cm^{-1} larger than that for the isoelectronic molecule YbOH [40, 41]. The energy difference $\sim 27 \text{ cm}^{-1}$ between $\nu_2 = 2^2$ and $\nu_2 = 2^0$ states is due to the anharmonicity of the potential and close to that for YbOH [41]. The l -doubling value for $\nu_2 = 1$ of 23.5 MHz is also close to that for YbOH . Based on our study in Ref. [40] we estimate the accuracy of the calculation on the level of 10%. The l -doubling for $\nu_2 = 2^2$ state is about three orders of magnitude smaller. This state can also be used for \mathcal{CP} -violation searches and can be completely polarized by electric field of a few V/cm.

In Tables II and III the calculated polarizations P and hyperfine energy levels, respectively for the lowest $N = 1$ rotational level of the first excited $v = 1$ bending vibrational mode of the $^{175}\text{LuOH}^+$ for the external electric fields $E = 50, 100, 150, 200, 250, 300, 350 \text{ V/cm}$ are presented. The selected values are comfortable for the experiment and ensure almost saturated values for polarizations. The levels are ordered by the energy value. Here $M_F = M_J + M_I^{\text{H}} + M_I^{\text{Lu}}$ is the projection of the total molecular (electronic-rotational-vibrational-nuclear spins) angular momentum \mathbf{F} on the lab axis. There are 24 levels for $M_F = 1/2$ and $M_F = 3/2$, 22 levels for $M_F = 5/2$, 16 levels for $M_F = 7/2$, 8 levels for $M_F = 9/2$ and 2 levels for $M_F = 11/2$. Calculations showed that all levels have polarizations $P < 0.6$. No level approaches $P = 1$ value in accordance to Ref. [13].

In Fig. 3 the calculated energies and P for the group of levels with zero field energy of $\sim 31850 \text{ MHz}$ as functions of the external electric field are presented. The selected states are appropriate for experiment. They have the largest polarizations, and it is the energy grouping with the fewest number of states (only 14). There are almost degenerate states with close values of P . These states differ by only projection $M_I^{\text{H}} = \pm 1/2$ which almost does not influence energy and P due to the weakness of the hyperfine interaction with hydrogen nucleus. Two states

⁴ We would like to mention again that these parameters are Jacobi coordinates, defined above; R is not the Lu-O distance.

with almost zero sensitivity to $e\text{EDM}$ have close to zero projection of total less hydrogen nuclear spin $M_J + M_I^{\text{Lu}}$ on the lab axis.

Finally we calculated vibrational energy levels and l -doubling effect for the first two bending excitation modes, hyperfine energy and sensitivity to $e\text{EDM}$ and the scalar-pseudoscalar nucleus-electron interaction, given by Eq. (1), for all hyperfine levels of the first excited bending mode of $^{175}\text{LuOH}^+$. Calculations are required for preparation and interpretation of the experiment on \mathcal{T}, \mathcal{P} -violation searches on $^{175}\text{LuOH}^+$.

Since LuOH^+ can be created by reacting laser-cooled atomic Lu+ ions with molecules containing an OH group (e.g., water), it is an ideal candidate molecule to use in a quantum logic spectroscopy type experiment, as detailed in [42]. With this experimental design, it should be possible to obtain a measurement precision of $15 \mu\text{Hz}$ in 300 hours of measurement with 12 molecular ions in an external electric field of 32 V/cm . This electric field corresponds to a polarization of 0.35 for co-magnetometer states 44 and 56 with $M_F = 5/2, 7/2$. These parameters yield a 1σ $e\text{EDM}$ precision of $3 \cdot 10^{-30} e \cdot \text{cm}$, which matches the precision of the most recent ACME measurement [6].

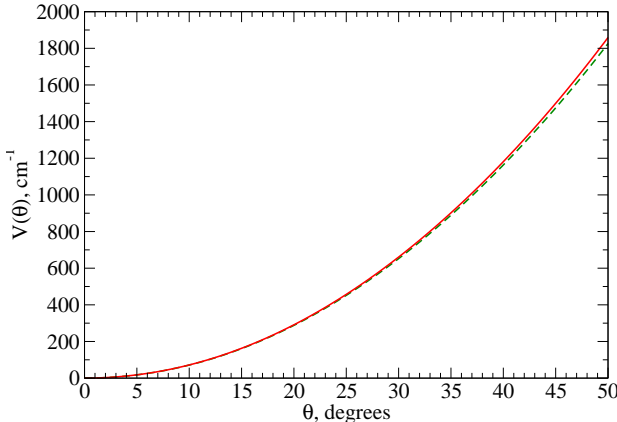


FIG. 2. Potential curve $V(\theta)$. Red (solid) curve is for CCSD, green (dashed) curve is for CCSD(T) calculations.

Electronic structure calculations have been carried out using computing resources of the federal collective usage center Complex for Simulation and Data Processing for Mega-science Facilities at National Research Centre “Kurchatov Institute”, <http://ckp.nrcki.ru/>.

Molecular rovibrational structure calculations have been supported by the Russian Science Foundation Grant No. 18-12-00227. Calculations of property integrals were supported by the Foundation for the Advancement of Theoretical Physics and Mathematics “BASIS” Grant according to Projects No. 20-1-5-76-1 and No. 21-1-2-47-1.

TABLE I. Calculated vibrational energy levels (cm^{-1}) and l -doubling (MHz) for the $\nu_2 = 0 - 2$ quanta of bending excitation modes of $^{175}\text{LuOH}^+$. Stretching mode ν_1 and ligand mode ν_3 quanta are zero in calculations.

Parameter	CCSD	CCSD(T)
$\nu_2 = 0$	0.	0.
$\nu_2 = 1$	445.	442.
$\nu_2 = 2^0$	878.	871.
$\nu_2 = 2^2$	904.	898.
l -doubling ($\nu_2 = 1$)	23.4	23.5
l -doubling ($\nu_2 = 2^2$)	0.005	0.005

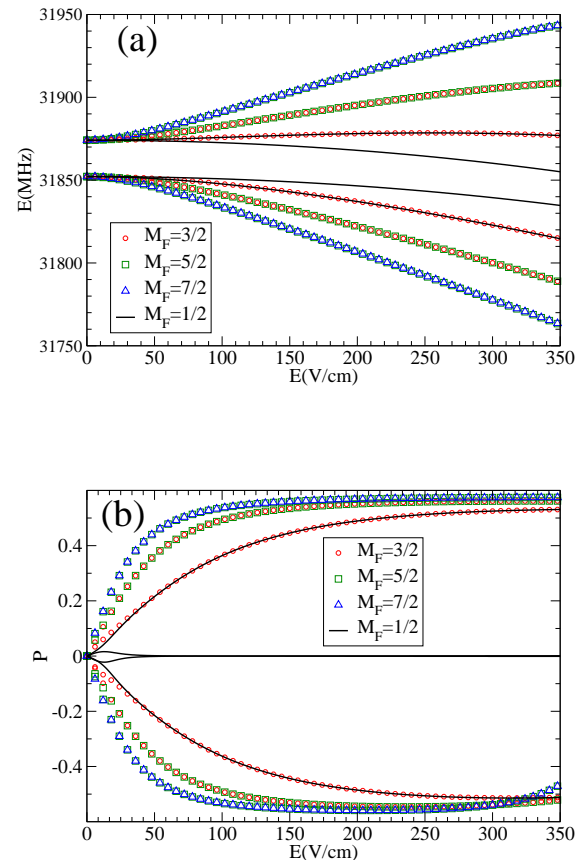


FIG. 3. (Color online) Energy (panel (a)) and polarization (panel(b)) for the group of levels with zero field energy of $\sim 31850 \text{ MHz}$, numbered 43-56.

* daniel.maison@gmail.com, maison_de@pnpi.nrcki.ru

† skripnikov_lv@pnpi.nrcki.ru, leonidos239@gmail.com

‡ glebpenyazkov@gmail.com

§ mgraub@odu.edu

¶ petrov_an@pnpi.nrcki.ru

TABLE II. The calculated polarizations P for the different projections of the total angular momentum M_F of the lowest $N = 1$ rotational level of the first excited the $v = 1$ bending vibrational mode of $^{175}\text{LuOH}^+$ for selected values of the external electric field (in V/cm). Levels are numbered by increasing energy given in Table III.

Electric field								Electric field									
#	M_F	50.	100.	150.	200.	250.	300.	350.	#	M_F	50.	100.	150.	200.	250.	300.	350.
1	1.5	-0.3811	-0.4750	-0.5012	-0.5112	-0.5157	-0.5180	-0.5190	49	0.5	0.0014	-0.0001	-0.0004	-0.0006	-0.0008	-0.0010	-0.0011
2	2.5	-0.3812	-0.4750	-0.5012	-0.5112	-0.5157	-0.5180	-0.5190	50	0.5	-0.0013	0.0002	0.0005	0.0006	0.0008	0.0010	0.0011
3	0.5	-0.2436	-0.3809	-0.4436	-0.4735	-0.4889	-0.4971	-0.5014	51	0.5	-0.2151	-0.3626	-0.4434	-0.4855	-0.5061	-0.5138	-0.5123
4	1.5	-0.2450	-0.3811	-0.4437	-0.4736	-0.4890	-0.4972	-0.5014	52	1.5	-0.2164	-0.3625	-0.4432	-0.4853	-0.5060	-0.5137	-0.5122
5	0.5	-0.0013	-0.0004	-0.0004	-0.0005	-0.0006	-0.0008	-0.0009	53	1.5	-0.3631	-0.4904	-0.5307	-0.5443	-0.5461	-0.5389	-0.5204
6	0.5	0.0011	0.0004	0.0004	0.0005	0.0007	0.0008	0.0009	54	2.5	-0.3631	-0.4903	-0.5306	-0.5442	-0.5460	-0.5388	-0.5203
7	1.5	0.2448	0.3807	0.4427	0.4713	0.4834	0.4835	0.4697	55	2.5	-0.4457	-0.5331	-0.5540	-0.5591	-0.5563	-0.5396	-0.4656
8	0.5	0.2436	0.3804	0.4426	0.4712	0.4833	0.4834	0.4696	56	3.5	-0.4457	-0.5330	-0.5539	-0.5590	-0.5562	-0.5395	-0.4656
9	2.5	0.3808	0.4741	0.4994	0.5059	-0.3943	-0.3964	-0.3968	57	4.5	0.3530	0.4008	0.4123	0.4169	0.4194	0.4209	0.4221
10	1.5	0.3807	0.4741	0.4994	0.5059	0.4797	-0.0144	-0.3131	58	5.5	0.3528	0.4006	0.4121	0.4167	0.4191	0.4207	0.4219
11	4.5	-0.3374	-0.3830	-0.3938	-0.3980	-0.4001	-0.4013	-0.4022	59	3.5	0.3266	0.3896	0.4054	0.4108	0.4128	0.4134	0.4133
12	3.5	-0.3374	-0.3830	-0.3938	-0.3980	-0.4000	-0.4013	-0.4021	60	4.5	0.3265	0.3894	0.4052	0.4106	0.4126	0.4132	0.4131
13	3.5	-0.3040	-0.3691	-0.3863	-0.3926	-0.3953	-0.3964	-0.3968	61	2.5	0.2853	0.3692	0.3934	0.4009	0.4001	0.3858	0.3149
14	2.5	-0.3039	-0.3691	-0.3862	-0.3925	0.4790	-0.0129	-0.3131	62	3.5	0.2853	0.3691	0.3932	0.4007	0.4000	0.3857	0.3148
15	1.5	-0.2449	-0.3369	-0.3678	-0.3775	-0.3531	0.1399	0.4377	63	1.5	0.2203	0.3258	0.3670	0.3829	0.3869	0.3821	0.3663
16	2.5	-0.2452	-0.3370	-0.3679	-0.3775	-0.3533	0.1384	0.4377	64	2.5	0.2205	0.3257	0.3668	0.3828	0.3868	0.3819	0.3662
17	0.5	-0.1419	-0.2446	-0.3027	-0.3338	-0.3488	-0.3511	-0.3388	65	0.5	0.1202	0.2201	0.2839	0.3216	0.3419	0.3503	0.3499
18	1.5	-0.1446	-0.2450	-0.3028	-0.3339	-0.3488	-0.3511	-0.3388	66	1.5	0.1241	0.2203	0.2837	0.3213	0.3417	0.3501	0.3497
19	0.5	-0.0024	-0.0004	-0.0002	-0.0002	-0.0003	-0.0003	-0.0004	67	0.5	0.0036	0.0002	-0.0003	-0.0005	-0.0006	-0.0008	-0.0009
20	0.5	0.0020	0.0003	0.0002	0.0002	0.0003	0.0003	0.0004	68	0.5	-0.0035	-0.0002	0.0003	0.0005	0.0006	0.0007	0.0008
21	0.5	0.1422	0.2444	0.3025	0.3343	0.3516	0.3609	0.3653	69	0.5	-0.1200	-0.2195	-0.2827	-0.3199	-0.3401	-0.3496	-0.3523
22	1.5	0.1444	0.2448	0.3026	0.3344	0.3517	0.3609	0.3653	70	1.5	-0.1238	-0.2197	-0.2825	-0.3197	-0.3399	-0.3494	-0.3522
23	1.5	0.2447	0.3364	0.3673	0.3794	0.3843	0.3858	0.3854	71	1.5	-0.2198	-0.3246	-0.3647	-0.3796	-0.3835	-0.3820	-0.3773
24	2.5	0.2450	0.3365	0.3674	0.3794	0.3843	0.3858	0.3854	72	2.5	-0.2201	-0.3245	-0.3646	-0.3795	-0.3834	-0.3819	-0.3772
25	2.5	0.3036	0.3683	0.3850	0.3907	0.3927	0.3929	0.3921	73	2.5	-0.2847	-0.3676	-0.3902	-0.3961	-0.3953	-0.3911	-0.3847
26	3.5	0.3036	0.3684	0.3850	0.3908	0.3927	0.3929	0.3921	74	3.5	-0.2847	-0.3674	-0.3901	-0.3959	-0.3952	-0.3909	-0.3845
27	4.5	0.3369	0.3821	0.3924	0.3961	0.3978	0.3985	0.3989	75	3.5	-0.3257	-0.3876	-0.4017	-0.4047	-0.4033	-0.3993	-0.3932
28	3.5	0.3369	0.3821	0.3924	0.3961	0.3977	0.3985	0.3989	76	4.5	-0.3256	-0.3874	-0.4015	-0.4045	-0.4031	-0.3991	-0.3930
29	2.5	0.0456	0.0794	0.1002	0.1122	0.1191	0.1230	0.1252	77	4.5	-0.3520	-0.3988	-0.4093	-0.4128	-0.4143	-0.4148	-0.4149
30	3.5	0.0457	0.0794	0.1001	0.1122	0.1191	0.1230	0.1252	78	5.5	-0.3518	-0.3985	-0.4091	-0.4126	-0.4140	-0.4146	-0.4147
31	1.5	0.0312	0.0585	0.0794	0.0946	0.1052	0.1127	0.1181	79	3.5	0.0082	0.0150	0.0201	0.0241	0.0273	0.0302	0.0328
32	2.5	0.0314	0.0585	0.0794	0.0946	0.1052	0.1127	0.1181	80	4.5	0.0083	0.0150	0.0202	0.0242	0.0274	0.0303	0.0329
33	0.5	0.0145	0.0311	0.0456	0.0586	0.0699	0.0797	0.0881	81	3.5	0.0063	0.0119	0.0164	0.0197	0.0217	0.0227	0.0225
34	1.5	0.0162	0.0315	0.0458	0.0587	0.0700	0.0798	0.0881	82	2.5	0.0062	0.0118	0.0163	0.0196	0.0217	0.0226	0.0224
35	0.5	0.0016	0.0003	0.0001	0.0001	0.0001	0.0001	0.0001	83	1.5	0.0039	0.0082	0.0119	0.0150	0.0172	0.0185	0.0189
36	0.5	-0.0063	-0.0032	-0.0011	-0.0005	-0.0003	-0.0002	-0.0002	84	2.5	0.0044	0.0083	0.0120	0.0150	0.0173	0.0186	0.0189
37	0.5	-0.0099	-0.0285	-0.0450	-0.0583	-0.0695	-0.0788	-0.0863	85	0.5	0.0014	0.0040	0.0063	0.0085	0.0106	0.0125	0.0142
38	1.5	-0.0195	-0.0322	-0.0462	-0.0589	-0.0699	-0.0790	-0.0865	86	1.5	0.0025	0.0043	0.0065	0.0086	0.0107	0.0126	0.0142
39	1.5	-0.0285	-0.0588	-0.0801	-0.0952	-0.1055	-0.1121	-0.1163	87	0.5	0.0007	0.0003	0.0001	0.0001	0.0000	0.0000	0.0000
40	2.5	-0.0331	-0.0593	-0.0803	-0.0953	-0.1055	-0.1129	-0.1273	88	3.5	-0.0056	-0.0120	-0.0171	-0.0213	-0.0258	-0.0311	-0.0374
41	3.5	-0.0463	-0.0805	-0.1018	-0.1142	-0.1214	-0.1253	-0.1273	89	4.5	-0.0069	-0.0126	-0.0172	-0.0214	-0.0259	-0.0312	-0.0375
42	2.5	-0.0450	-0.0804	-0.1018	-0.1142	-0.1213	-0.1246	-0.1164	90	2.5	-0.0041	-0.0089	-0.0150	-0.0204	-0.0259	-0.0320	-0.0387
43	2.5	0.4474	0.5366	0.5597	0.5684	0.5722	0.5739	0.5746	91	3.5	-0.0066	-0.0110	-0.0155	-0.0205	-0.0260	-0.0321	-0.0387
44	3.5	0.4473	0.5365	0.5597	0.5683	0.5721	0.5739	0.5746	92	0.5	-0.0008	-0.0018	-0.0028	-0.0031	-0.0021	-0.0010	-0.0004
45	1.5	0.3642	0.4928	0.5350	0.5515	0.5586	0.5613	0.5618	93	1.5	-0.0025	-0.0054	-0.0091	-0.0134	-0.0179	-0.0222	-0.0260
46	2.5	0.3642	0.4927	0.5349	0.5515	0.5585	0.5613	0.5617	94	0.5	-0.0010	-0.0021	-0.0037	-0.0067	-0.0116	-0.0171	-0.0223
47	0.5	0.2156	0.3638	0.4457	0.4894	0.5128	0.5252	0.5309	95	1.5	-0.0030	-0.0061	-0.0094	-0.0132	-0.0180	-0.0238	-0.0306
48	1.5	0.2170	0.3637	0.4455	0.4892	0.5127	0.5251	0.5308	96	2.5	-0.0049	-0.0091	-0.0124	-0.0169	-0.0222	-0.0280	-0.0339

TABLE III. The calculated energies (in MHz) for the different projections of the total angular momentum M_F of the lowest $N = 1$ rotational level of the first excited $v = 1$ bending vibrational mode of $^{175}\text{LuOH}^+$ for the selected values of the external electric field (in V/cm). Levels are numbered by the increasing energy. Zero energy level corresponds to the lowest energy of $N = 1$ states at zero electric field.

Electric field										Electric field									
#	M_F	50.	100.	150.	200.	250.	300.	350.	#	M_F	50.	100.	150.	200.	250.	300.	350.		
1	1.5	-5	-16	-28	-41	-54	-68	-82	49	0.5	31852	31851	31849	31847	31843	31839	31835		
2	2.5	-5	-16	-28	-41	-55	-68	-82	50	0.5	31874	31873	31871	31868	31864	31860	31855		
3	0.5	-2	-6	-12	-19	-27	-35	-44	51	0.5	31875	31876	31877	31878	31879	31878	31877		
4	1.5	-2	-6	-12	-19	-27	-35	-44	52	1.5	31875	31876	31877	31878	31879	31878	31877		
5	0.5	0	-1	-2	-4	-6	-9	-13	53	1.5	31877	31883	31889	31895	31901	31905	31909		
6	0.5	23	23	21	19	17	14	10	54	2.5	31877	31883	31889	31895	31901	31905	31909		
7	1.5	25	28	32	35	38	41	43	55	2.5	31880	31891	31903	31914	31925	31935	31944		
8	0.5	25	28	32	35	39	41	43	56	3.5	31880	31891	31903	31914	31925	31936	31944		
9	2.5	29	39	49	60	69	55	41	57	4.5	32043	32027	32010	31992	31974	31956	31938		
10	1.5	29	39	49	60	70	75	66	58	5.5	32043	32027	32010	31992	31974	31956	31939		
11	4.5	119	102	85	67	49	31	13	59	3.5	32046	32033	32019	32004	31988	31973	31957		
12	3.5	119	102	85	67	49	32	14	60	4.5	32046	32033	32019	32004	31988	31973	31957		
13	3.5	122	110	97	83	69	55	40	61	2.5	32048	32039	32028	32016	32003	31991	31980		
14	2.5	122	111	97	84	70	74	66	62	3.5	32049	32039	32028	32016	32003	31991	31980		
15	1.5	125	118	109	100	90	86	93	63	1.5	32051	32045	32037	32028	32019	32009	32000		
16	2.5	125	118	109	100	90	86	93	64	2.5	32051	32045	32037	32028	32019	32009	32000		
17	0.5	128	125	121	116	110	104	99	65	0.5	32052	32049	32045	32040	32033	32027	32020		
18	1.5	128	125	121	116	110	104	99	66	1.5	32052	32049	32045	32040	32034	32027	32020		
19	0.5	128	128	127	125	123	121	119	67	0.5	32053	32051	32049	32046	32043	32039	32035		
20	0.5	152	151	150	148	146	144	142	68	0.5	32076	32074	32072	32068	32064	32060	32055		
21	0.5	153	154	156	158	160	162	164	69	0.5	32076	32076	32076	32075	32074	32073	32071		
22	1.5	153	154	156	158	160	162	164	70	1.5	32076	32076	32076	32075	32074	32073	32071		
23	1.5	155	161	168	175	182	189	195	71	1.5	32078	32081	32085	32089	32091	32094	32096		
24	2.5	155	161	168	175	182	189	195	72	2.5	32078	32081	32085	32089	32091	32094	32096		
25	2.5	158	169	182	194	206	218	230	73	2.5	32080	32088	32096	32103	32111	32117	32123		
26	3.5	158	169	181	194	206	218	230	74	3.5	32080	32088	32096	32103	32111	32117	32123		
27	4.5	162	178	195	213	231	249	267	75	3.5	32083	32095	32107	32120	32132	32143	32154		
28	3.5	162	178	196	213	231	249	267	76	4.5	32083	32095	32107	32120	32132	32143	32154		
29	2.5	689	687	685	682	680	677	674	77	4.5	32086	32102	32119	32137	32155	32172	32190		
30	3.5	689	687	685	683	680	677	674	78	5.5	32086	32102	32120	32137	32155	32173	32190		
31	1.5	689	689	690	690	691	692	694	79	3.5	32320	32319	32317	32316	32314	32313	32311		
32	2.5	689	689	690	690	691	692	694	80	4.5	32320	32319	32317	32316	32314	32312	32311		
33	0.5	690	691	693	695	699	703	707	81	3.5	32320	32321	32322	32323	32325	32328	32331		
34	1.5	690	691	693	695	699	703	707	82	2.5	32320	32321	32322	32323	32325	32328	32331		
35	0.5	690	691	694	697	701	707	713	83	1.5	32321	32323	32325	32329	32334	32339	32346		
36	0.5	713	715	717	720	724	729	735	84	2.5	32321	32322	32325	32329	32334	32339	32346		
37	0.5	714	715	717	721	725	730	736	85	0.5	32321	32323	32327	32333	32339	32347	32355		
38	1.5	713	715	717	721	725	730	736	86	1.5	32321	32323	32327	32333	32339	32347	32355		
39	1.5	714	715	718	722	726	732	738	87	0.5	32321	32324	32328	32334	32341	32350	32359		
40	2.5	714	715	718	722	727	732	737	88	3.5	32342	32344	32347	32351	32356	32362	32368		
41	3.5	714	716	719	723	727	732	737	89	4.5	32342	32344	32347	32351	32356	32362	32368		
42	2.5	714	716	719	723	727	732	738	90	2.5	32342	32344	32348	32353	32359	32366	32374		
43	2.5	31846	31834	31820	31806	31792	31778	31763	91	3.5	32342	32344	32348	32353	32359	32366	32374		
44	3.5	31846	31834	31821	31807	31792	31778	31763	92	0.5	32342	32344	32348	32353	32360	32368	32376		
45	1.5	31849	31841	31832	31822	31811	31800	31788	93	1.5	32342	32344	32348	32353	32360	32368	32377		
46	2.5	31849	31841	31832	31822	31811	31800	31789	94	0.5	32342	32345	32348	32354	32360	32368	32377		
47	0.5	31851	31848	31843	31837	31830	31823	31815	95	1.5	32342	32345	32348	32354	32360	32368	32377		
48	1.5	31851	31848	31843	31837	31830	31823	31815	96	2.5	32342	32345	32348	32353	32360	32368	32377		

- ** <http://www.qchem.pnpi.spb.ru>
- [1] M. S. Safranova, D. Budker, D. DeMille, D. F. J. Kimball, A. Derevianko, and C. W. Clark, Rev. Mod. Phys. **90**, 025008 (2018).
 - [2] A. D. Sakharov, JETP lett. **5**, 24 (1967).
 - [3] R. Alarcon, J. Alexander, V. Anastassopoulos, T. Aoki, R. Baartman, S. Baeßler, L. Bartoszek, D. H. Beck, F. Bedeschi, R. Berger, et al., *Electric dipole moments and the search for new physics* (2022), URL <https://arxiv.org/abs/2203.08103>.
 - [4] C. Abel, S. Afach, N. J. Ayres, C. A. Baker, G. Ban, G. Bison, K. Bodek, V. Bondar, M. Burghoff, E. Chanel, et al., Phys. Rev. Lett. **124**, 081803 (2020).
 - [5] M. Swallows, T. Loftus, W. Griffith, B. Heckel, E. Fortson, and M. V. Romalis, Physical Review A **87**, 012102 (2013).
 - [6] V. Andreev, D. Ang, D. DeMille, J. Doyle, G. Gabrielse, J. Haefner, N. Hutzler, Z. Lasner, C. Meisenhelder, B. O’Leary, et al., Nature **562**, 355 (2018).
 - [7] J. Baron, W. C. Campbell, D. DeMille, J. M. Doyle, G. Gabrielse, Y. V. Gurevich, P. W. Hess, N. R. Hutzler, E. Kirilov, I. Kozyryev, et al. (The ACME Collaboration), Science **343**, 269 (2014).
 - [8] W. B. Cairncross, D. N. Gresh, M. Grau, K. C. Cossel, T. S. Roussy, Y. Ni, Y. Zhou, J. Ye, and E. A. Cornell, Phys. Rev. Lett. **119**, 153001 (2017).
 - [9] I. B. Khriplovich and S. K. Lamoreaux, *CP Violation without Strangeness. The Electric Dipole Moments of Particles, Atoms, and Molecules* (Springer-Verlag, Berlin, 1997).
 - [10] Y. Yamaguchi and N. Yamanaka, Phys. Rev. D **103**, 013001 (2021).
 - [11] I. Kozyryev and N. R. Hutzler, Phys. Rev. Lett. **119**, 133002 (2017).
 - [12] T. A. Isaev, A. V. Zaitsevskii, and E. Eliav, J. Phys. B: At. Mol. Opt. Phys. **50**, 225101 (2017).
 - [13] A. Petrov and A. Zakharova, Phys. Rev. A **105**, L050801 (2022), URL <https://link.aps.org/doi/10.1103/PhysRevA.105.L050801>.
 - [14] B. L. Augenbraun, Z. D. Lasner, A. Frenett, H. Sawaoka, C. Miller, T. C. Steimle, and J. M. Doyle, New J. Phys. (2020).
 - [15] D. E. Maison, L. V. Skripnikov, V. V. Flambaum, and M. Grau, J. Chem. Phys. **153**, 224302 (2020).
 - [16] R. Kaewuam, A. Roy, T. R. Tan, K. J. Arnold, and M. D. Barrett, Journal of Modern Optics **65**, 592 (2018).
 - [17] A.-M. Mårtensson-Pendrill and P. Öster, Phys. Scr. **36**, 444 (1987).
 - [18] E. Lindroth, B. W. Lynn, and P. G. H. Sandars, J. Phys. B **22**, 559 (1989).
 - [19] I. B. Khriplovich, *Parity non-conservation in atomic phenomena* (Gordon and Breach, New York, 1991).
 - [20] J. S. M. Ginges and V. V. Flambaum, Phys. Rep. **397**, 63 (2004).
 - [21] O. P. Sushkov and V. V. Flambaum, Sov. Phys. – JETP **48**, 608 (1978).
 - [22] K. C. Cossel, D. N. Gresh, L. C. Sinclair, T. Coffey, L. V. Skripnikov, A. N. Petrov, N. S. Mosyagin, A. V. Titov, R. W. Field, E. R. Meyer, et al., Chem. Phys. Lett. **546**, 1 (2012).
 - [23] T. D. Crawford and H. F. Schaefer III, Rev. Comput. Chem. **14**, 33 (2000).
 - [24] R. J. Bartlett, Theoretica chimica acta **80**, 71 (1991).
 - [25] R. J. Bartlett and M. Musiał, Rev. Mod. Phys. **79**, 291 (2007).
 - [26] A. S. P. Gomes, K. G. Dyall, and L. Visscher, Theor. Chim. Acta **127**, 369 (2010).
 - [27] T. H. Dunning, Jr, J. Chem. Phys. **90**, 1007 (1989).
 - [28] R. A. Kendall, T. H. Dunning, Jr, and R. J. Harrison, J. Chem. Phys. **96**, 6796 (1992).
 - [29] K. G. Dyall, Theor. Chem. Acc. **135**, 128 (2016).
 - [30] L. V. Skripnikov, D. E. Maison, and N. S. Mosyagin, Phys. Rev. A **95**, 022507 (2017).
 - [31] L. V. Skripnikov and A. V. Titov, J. Chem. Phys. **142**, 024301 (2015).
 - [32] DIRAC, a relativistic ab initio electronic structure program, Release DIRAC19 (2019), written by A. S. P. Gomes, T. Saué, L. Visscher, H. J. Aa. Jensen, and R. Bast, with contributions from I. A. Aucar, V. Bakken, K. G. Dyall, S. Dubillard, U. Ekstroem, E. Eliav, T. Enevoldsen, E. Fasshauer, T. Fleig, O. Fossgaard, L. Halbert, E. D. Hedegaard, T. Helgaker, J. Henriksson, M. Ilias, Ch. R. Jacob, S. Knecht, S. Komorovsky, O. Kullie, J. K. Laerdahl, C. V. Larsen, Y. S. Lee, H. S. Nataraj, M. K. Nayak, P. Norman, M. Olejniczak, J. Olsen, J. M. H. Olsen, Y. C. Park, J. K. Pedersen, M. Pernpointner, R. Di Remigio, K. Ruud, P. Salek, B. Schimmelpfennig, B. Senjean, A. Shee, J. Sikkema, A. J. Thorvaldsen, J. Thyssen, J. van Stralen, M. L. Vidal, S. Villaume, O. Visser, T. Winther, and S. Yamamoto (see <http://diracprogram.org>). (accessed on 4 February 2022).
 - [33] R. Saué, T. Bast, A. S. P. Gomes, H. J. A. Jensen, L. Visscher, I. A. Aucar, R. Di Remigio, K. G. Dyall, E. Eliav, E. Fasshauer, T. Fleig, et al., J. Chem. Phys. **152**, 204104 (2020).
 - [34] L. V. Skripnikov, J. Chem. Phys. **145**, 214301 (2016).
 - [35] L. V. Skripnikov, A. V. Titov, and V. V. Flambaum, Phys. Rev. A **95**, 022512 (2017).
 - [36] L. D. Landau and E. M. Lifshitz, *Quantum mechanics* (Pergamon, Oxford, 1977), 3rd ed.
 - [37] A. N. Petrov, Phys. Rev. A **83**, 024502 (2011).
 - [38] P. Pyykkö, Molecular Physics **106**, 1965 (2008).
 - [39] N. Stone, Table of nuclear magnetic dipole and electric quadrupole moments, INDC(NDS)-0658, International Atomic Energy Agency (IAEA) (2014).
 - [40] A. Zakharova and A. Petrov, J. Chem. Phys. **157**, 154310 (2022).
 - [41] C. Zhang, B. L. Augenbraun, Z. D. Lasner, N. B. Vilas, J. M. Doyle, and L. Cheng, The Journal of Chemical Physics **155**, 091101 (2021).
 - [42] T. N. Taylor, J. O. Island, and Y. Zhou, *Quantum logic control and precision measurements of molecular ions in a ring trap – a new approach for testing fundamental symmetries* (2022), URL <https://arxiv.org/abs/2210.11613>.